Life-cycle analysis of shared e-scooter: data-driven approaches in 100 EU cities

Transportation Research Part D 148 (2025) 105009

Contents lists available at ScienceDirect

Transportation Research Part D

journal homepage: www.elsevier.com/locate/trd

Life-cycle analysis of shared e-scooter: Data-driven approaches in 100 EU cities

Ruo Jia, Kun Gao *

Department of Architecture and Civil Engineering, Chalmers University of Technology, SE-412 96, Gothenburg, Sweden

ARTICLE INFO

Keywords:
Shared micro-mobility
E-scooter
Life cycle assessment
Greenhouse gas

ABSTRACT

While shared electric scooter (SES) systems continue to expand, their environmental sustainability remains contested due to limited existing assessments that predominantly employ static emission factors and idealized operational assumptions. Using SES data and electricity-mix generation profiles across 100 EU cities, we estimate greenhouse gas emissions for SES through a life cycle assessment approach. Manufacturing, shipping, and end-of-life collectively impose a fixed burden of 115.6 kg CO2eq per scooter. Operational data reveals dynamic consumption patterns, with active riding averaging 15.9 Wh km-1 and idle-phase drawing 1.5 W. Applying usage patterns derived from empirical data, total emission factors range from 30 to 124 g CO2-eq km-1, influenced primarily by trip frequency, distance, and the carbon intensity of electricity generation. Comparative analyses at city and country levels, along with sensitivity assessments, indicate that enhancing utilization rates and decarbonizing electricity supplies are pivotal strategies for achieving climate-neutral shared e-scooter systems.

1. Introduction

The rise of shared electric scooters (SES) has transformed urban mobility in cities across Europe and globally, offering a flexible and on-demand mode of transport that promises to reduce congestion, complement public transit, and decrease the reliance on private vehicles (Baumgartner and Helmers, 2024; Gao et al., 2024). As SES schemes become increasingly implemented within the urban transport contexts of different cities, their environmental credentials have attracted significant attention from policymakers, researchers, and the public (Liu et al., 2023; Jia et al., 2023). Advocates of SES highlight their potential as a low-carbon alternative for short-distance trips, positioning them as a pivotal solution for sustainable urban mobility transitions (Hu et al., 2025; Gao et al., 2021b). However, the true environmental impact of SES remains a subject of active debate. Most existing environmental assessments are grounded in modeled or assumed emission factors of SES, drawing on generic life cycle inventory (LCI) data and arbitrary assumptions of usage patterns. While such approaches provide preliminary benchmarks, they fall short in capturing the complex realities of SES operations, which are subject to considerable spatial and operational heterogeneity (Gao et al., 2021a; Calan et al., 2024). This lack of empirical specificity from field big data of SES has led to inconsistent findings regarding the life cycle emission factors and the overall climate benefits of SES.

Crucially, life cycle assessment (LCA) studies have reported a wide spectrum of results for SES systems. Several comprehensive analyses indicate that upstream phases, manufacturing, logistics, and end-of-life processing, can account for the majority (up to 80%) of total greenhouse gas (GHG) emissions associated with SES fleets (Calan et al., 2024; Moreau et al., 2020). Conversely, the

* Corresponding author at: Sven Hultins Gata 6, Goteborg, Sweden
E-mail address: gkun@chalmers.se (K. Gao).

https://doi.org/10.1016/j.trd.2025.105009
Received 7 June 2025; Received in revised form 5 August 2025; Accepted 18 September 2025
Available online 7 October 2025

Nomenclature

CO_2-eq	CO_2-equivalent
GHG	Greenhouse gas emission
GWP	Global warming potential
LCA	Life cycle assessment
LCI	Life cycle inventor
SES	Shared electric scooter

operational phase, particularly in regions with decarbonized electricity grids, has been shown to contribute a much smaller share (Baumgartner and Helmers, 2024; European Environment Agency, 2024). These studies underscore the importance of considering the entire value chain, from raw material extraction and vehicle assembly to daily fleet operations and eventual disposal.

Nonetheless, several critical limitations persist in this field. Most LCAs of SES employ static and country-average values for grid carbon intensity, neglecting the substantial temporal and spatial variability that can arise from shifts in electricity generation mix and demand (European Environment Agency, 2024; Brandt et al., 2024). This simplification may mask important differences in emissions associated with SES charging activities. Furthermore, empirical data on operational realities such as actual scooter lifespans, maintenance frequency, idle-time energy use, and real user trip patterns, are often lacking or replaced by stylized and arbitrary assumptions, limiting the accuracy of life cycle emission estimates (Su et al., 2024). Recent improvements in vehicle design and operational practices, including enhanced maintenance and battery swapping, have increased lifespans and reduced emissions, yet these developments are not always incorporated into assessment models. Moreover, previous research seldom integrates high-resolution operational data with granular and country-specific electricity carbon intensity in a unified framework, and the contribution of idle-phase energy losses remains underexplored despite potentially significant impacts on overall emissions. Together, these gaps hinder reliable and context-sensitive quantification of the life cycle emission and impacts of SES, which potentially obscures key opportunities for emission reduction across the value chain (Li et al., 2024; Kuang et al., 2024; Kolat et al., 2023). Summarily, these limitations highlight a persistent gap in quantification of SES life cycle emissions based on field operation data of SES. There is an need for a comprehensive and data-driven LCA framework and empirical analysis that account for the temporal and spatial heterogeneity of electricity supply, usage patterns and the full operational life cycle of SES fleets from field data. Addressing these complexities can help policymakers and operators make informed decisions to optimize environmental outcomes and realize the sustainable mobility potential of SES.

To address these gaps, this study poses the following research questions:

1. How do country-level variations in electricity-grid carbon intensity influence the life cycle emissions and emission factors (measured by CO_2-eq km^{-1}) of SES?
2. To what extent do empirical operational usage patterns (including trip distance, usage frequency and energy loses during idling) in different cities affect the life cycle emissions and emission factors of SES?

To address the research questions, this study proposes a discrete-event and big-data-driven life cycle assessment of SES systems (overall life cycle emissions and emission factors), utilizing operational data from 100 European cities along with country-specific records on electricity carbon intensity. Emissions are quantified across the full life cycle including production, transportation, in-use, idle, and end-of-life phases, while explicitly capturing the real-world operational dynamics unique to each urban context. By integrating large-scale and heterogeneous operation data, this study aims to offer the most comprehensive LCA of SES systems across Europe to date. The findings are expected to yield data-driven and reliable insights into the life cycle emissions of SES in diverse urban settings, thereby informing both policy and operational strategies for fostering the sustainable integration of SES into urban mobility systems.

The remainder of the paper is organized as follows. Section 2 reviews the literature on empirical LCA of SES and the effects of grid variability. Section 3 details our discrete-event life cycle inventor framework and data sources. Section 4 presents the multi-city operational datasets and the results of phase-specific and total life cycle emissions, along with a sensitivity analysis. Finally, Section 5 concludes with key findings, recommendations for optimizing SES life cycle emissions, and suggestions for future research.

2. Literature review

Existing studies and some shared micro-mobility operators have announced the life cycle emission factor with the designed process, targeting the average life cycle within several estimated life expectancies. However, early deployments were marked by very short operational lifespans and inefficient methods, leading to high life cycle emissions. More recent operational data from European cities demonstrate that interventions such as battery swapping, optimized collection routing, and enhanced maintenance protocols have both prolonged scooter lifespans and lowered their carbon footprints (Hollingsworth et al., 2019).

2.1. Life cycle assessment of SES

Various methodologies for quantifying the life cycle emissions of SES typically partition the assessment into four sequential phases including manufacturing (encompassing raw material extraction and component assembly), transportation (shipping and distribution logistics), use (operational electricity consumption) and end-of-life (waste treatment, recycling processes, and final disposal), thereby allowing a comprehensive assessment of emissions from cradle to grave.

2.1.1. Production

The production stage of SES encompasses the extraction and processing of raw materials (notably aluminum alloys, steel, and lithium-ion battery materials), as well as the manufacturing and assembly of scooter units. Nearly all studies concur that the production phase (also termed "materials and manufacturing") is the single largest contributor to life cycle emissions for SES. Manufacturing e-scooters has been found to account for approximately 50% to 70% of total life cycle GHG emissions (Baumgartner and Helmers, 2024; Hollingsworth et al., 2019). For example, Hollingsworth et al. (2019) reported manufacturing as about 50% of shared scooter life cycle emissions. A recent systematic review similarly concluded that materials and production typically constitute >60% of total emissions for SES (Calan et al., 2024). The high production footprint is primarily due to emissions embodied in key components. The aluminum frame, although providing a lightweight and strong structure, is energy-intensive to produce, contributing approximately 40%–65% of manufacturing-phase GHG emissions (Baumgartner and Helmers, 2024). Aluminum constitutes almost half of the mass of a scooter and dominates the impact of production, despite manufacturers increasingly using around 25% recycled aluminum content (Calan et al., 2024). The lithium-ion battery pack also significantly accounts for approximately 10%–20% of production emissions. For instance, aluminum and lithium-ion batteries together account for approximately 53%–73% of production-phase emissions (Calan et al., 2024). Moreau et al. (2020) similarly found material production dominant, constituting 68%–90% of total impacts in their Brussels case study (131g CO_2-eq/pkm), with aluminum frames and batteries being the main contributors.

2.1.2. Shipping

The shipping stage of SES encompasses fleet shipping logistics and vehicle movements required for deployment and maintenance. This includes initial shipment from manufacturing sites to operational cities, where transport modes (e.g., rail, sea freight and road) impart significantly different emissions (Zhu and Lu, 2023; Holmgren et al., 2024). It also includes regular collection of low-battery scooters, transfer to charging facilities, and subsequent redistribution within cities. Using fossil-fueled vehicles for these logistics can significantly contribute to life cycle emissions. In the U.S., Hollingsworth et al. (2019) found that collection and charging operations alone accounted for approximately 43% of total life cycle GHG emissions, nearly equaling manufacturing impacts. Contemporary European studies indicate considerable variability: integrated-battery systems require approximately 100 m of service-vehicle travel per scooter-km, while swappable-battery configurations reduce this to around 35 m per scooter-km (Holmgren et al., 2024). Fleet-vehicle travel distances in Paris and Berlin range from 0.02 km to 2.5 km per scooter-km, corresponding to emissions of approximately 5.5 to 54 g CO_2-eq km^{-1}, depending on operational strategies and utilization frequency (Calan et al., 2024). Minimizing collection distances or increasing scooter usage could significantly reduce life cycle emissions of SES.

2.1.3. Usage

The usage phase includes direct emissions primarily from electricity generation for battery charging. Compared to manufacturing and transportation, use-phase emissions are lower, particularly in European decarbonizing electricity context. Typical scooter models consume approximately 1.5 to 2 kWh per 100km (15 to 20 Wh km^{-1}). For instance, charging a scooter for a 5 km ride may require around 0.1 kWh (Calan et al., 2024). A Parisian case study showed negligible use-phase impact compared to other phases due to French nuclear-heavy electricity mix (Calan et al., 2024). Similarly, switching to fully renewable electricity would reduce emissions by only about 1 g CO_2-eq km^{-1}. In Sweden, charging is estimated at 0.016 kWh km^{-1} (Holmgren et al., 2024).

Charging emissions vary widely across European countries, reflecting significant spatial and temporal variability in electricity carbon intensity. Scarlat et al. (2022) found 2019 electricity intensity ranged from 26–40 g CO_2-eq/kWh in low-carbon grids (such as Norway, Sweden, France) to around 1000 g CO_2-eq/kWh in coal-heavy grids (such as Kosovo and Poland). These disparities underscore the importance of incorporating country-specific electricity emission factors into LCA of SES to accurately assess the environmental impacts of charging activities. Tranberg et al. (2019) highlighted the significant temporal fluctuations in electricity carbon intensity due to factors like renewable energy availability and demand patterns. Such temporal heterogeneity suggests that using annual average emission factors may mask critical variations, leading to potential inaccuracies in LCA results. In the context of SES operations, these findings imply that charging-related emissions can vary widely depending on geographic location and time. For instance, SES charging in countries with carbon-intensive electricity grids, such as Poland, leads to considerably higher emissions than in regions with low-carbon grids, such as Sweden or France (Holmgren et al., 2024). Therefore, integrating high-resolution, country-specific, and time-resolved electricity carbon intensity data into LCA of SES is crucial across Europe.

Furthermore, studies have shown that idle energy losses in SES operations can be substantial. For example, Li et al. (2022) observed that the majority of SES were reused after long idle durations, with only a small fraction being redeployed shortly after previous use, resulting in 32.9% of electricity wasted. These research highlight the importance of considering idle phase emissions in LCA of SES. Additionally, the environmental impact of SES operations is influenced by factors such as vehicle lifespan, maintenance, and redistribution practices. For example, a study conducted in Lisbon, Portugal, emphasized the significance of these factors in the overall environmental performance of SES. To accurately assess LCA of SES, it is crucial to consider idle phase electricity consumption, and account for operational factors such as vehicle lifespan and maintenance practices.

2.1.4. End of life

End-of-life (EoL) treatment of SES encompassing disassembly, material recovery, and disposal, influences their net life cycle GHG emissions by offsetting virgin material production through recycling credits. Early life cycle assessments often neglected or implicitly subsumed EoL impacts within manufacturing, thereby underestimating the benefits of material reclamation. In practice, European recycling infrastructures recover high-value metals (such as aluminum, steel, copper) and increasingly lithium-ion battery constituents, yielding significant emissions reductions. For example, Gebhardt et al. (2022) incorporated metal scrap recovery and

Table 1
End-of-life (EoL) share of total life cycle GHG emissions in selected studies.

Reference	Area	EoL Share
Kazmaier et al. (2020)	Germany	3.17 %
Schelte et al. (2021)	Germany	1.00 %
Reis et al. (2023)	Portugal	1.00 %
Dott (2024)	Europe	1.10 %

Table 2
Summary of lifespan for shared E-Scooters in Europe.

Reference	Assumed Lifetime	Notes
Hollingsworth et al. (2019)	0.5–1 year	US study; high rebalancing impact
Moreau et al. (2020)	0.78 years / 1400 km	Brussels case study
Dott (2024)	4 years	Europe
Baumgartner and Helmers (2024)	1.5–2 years	Optimized operations in Europe
Calan et al. (2024)	3 years / 4000 km	Latest generation; highly efficient
Voi (2025)	4.6–5 years	Optimized operations in Europe

battery recycling to moderate overall impacts, while Reis et al. (2023) estimated that recycling 10 % of battery materials and 83 % of powertrain components could halve life cycle GHG emissions relative to zero-recycling scenarios. Conversely, omitting all recycling can roughly double total emissions, underscoring the importance of EoL strategy. Table 1 summarises the proportion of total life cycle emissions attributed to the EoL stage in recent studies. Although the EoL contribution is generally modest—ranging from 0 % in Brussels (Weschke et al., 2022) to 3.17 % in Berlin (Kazmaier et al., 2020), even small improvements in recycling rates can yield meaningful absolute reductions in life cycle GHG emissions Table 2.

Furthermore, initiatives to harvest spare parts from decommissioned units further curtail waste streams and can augment material-recovery credits. As EU regulations and technologies advance (particularly under the EU Battery Directive) improving recovery rates for battery metals and other components, the per-scooter carbon intensity at end-of-life is expected to decline correspondingly. Aluminium, for instance, is highly recyclable with much lower energy requirements than primary production. Steel parts, copper wiring, and the lithium battery (which contains metals that can be recycled or down-cycled) all have some residual value. A few studies attempted to model these effects. Gebhardt et al. (2022) assumed that major metal components would be recovered as scrap and battery recycling would occur, thereby slightly reducing overall impacts (Calan et al., 2024). Reis et al. (2023)) went further to estimate that if about 10% of the lithium battery material and 83% of the powertrain (motor and metals) were recycled at EoL, the total life cycle GHG emissions could be cut by approximately 50% compared to no-recycling (Calan et al., 2024). Similarly, the effective recycling could provide roughly an 80% “recovery benefit” for e-scooter and e-bike materials (Calan et al., 2024). In the EU context, it is likely that end-of-life processes will capture some value: aluminum frames will almost certainly be scrapped and recycled, and initiatives for battery recycling (in line with EU Battery Directive requirements) are ramping up. Some operators have also explored re-using retired scooters for parts. For example, spare parts from decommissioned units can be harvested to repair other scooters (Calan et al., 2024), further reducing waste.

In summary, end-of-life management can mitigate the overall carbon footprint of shared e-scooters by recovering materials and reducing the need for new production. While this stage often receives less attention than production or use phases, it can meaningfully improve the life cycle balance. The degree of benefit depends on recycling technology and practices. As recycling rates for lithium batteries improve and more components are reclaimed, the net emissions per scooter will correspondingly decline.

2.2. Lifespan of SES

Besides, the life cycle emission factors (measured by CO_2-eq km^{-1}) of SES are highly contingent upon the total distance each vehicle travels over its service life. Because the substantial emissions incurred during manufacturing are allocated across all kilometers travelled, the per-kilometer carbon footprint declines sharply as lifespan increases. Conversely, limited usage or premature retirement concentrates those initial emissions and thus elevates the carbon intensity per kilometer. For example, Moreau et al. (2020) estimate that in Brussels, an average scooter service life of 284 days and a lifetime distance of roughly 1 400 km correspond to 131 g CO_2-eq km^{-1}. Similarly, Hollingsworth et al. (2019) demonstrate that extending the operational lifetime of a scooter from six months to two years reduces its life cycle emission factor from 202 g CO_2-eq per mile (126 g CO_2-eq km^{-1}) to 141 g CO_2-eq per mile (88 g CO_2-eq km^{-1}). In stark contrast, early scooter deployments in Lisbon characterized by an average service duration of only 45 days and approximately 90 km travelled, yielded an extreme carbon intensity of 803 g CO_2-eq per km (Calan et al., 2024). Since 2021, industry efforts to improve scooter durability have targeted service lives of 18 to 24 months, corresponding to several thousand kilometers, thereby driving down per-kilometer emissions. Under these enhanced durability scenarios, the latest European model, engineered for a three-year lifespan and an expected 4 000 km total distance—achieves approximately 57 g CO_2-eq km^{-1}, and a recent German study suggests that optimized logistics combined with a 15-month lifetime could reduce emissions to 46 g CO_2-eq km^{-1}

(Calan et al., 2024). Considering the SES industry has made notable strides in enhancing scooter lifespan, accounting for this factor in LCA models is crucial for precise LCA of SES.

2.3. Research Gap

Although the life cycle assessment of SES have attracted scholarly attention, several critical gaps remain in current literature. Notably, existing studies often rely on simplified assumptions regarding electricity carbon intensity and operational patterns of SES (in terms of trip distance, usage frequency and idling time/electricity consumption). These overlook the complexity and variability in this two key factors affecting LCA of SES systems across different city contexts. These oversights can significantly undermine the accuracy and generalizability of LCA outcomes.

First, there is a lack of estimating SES lifespan travelled kilometers using large-scale real-world trip data. Most prior assessments adopt assumed or averaged lifespan travelled kilometers values, which introduces substantial uncertainty in estimating per-kilometer GHG emission factors. Given the sensitivity of use-phase emissions and emission factors to lifespan travelled kilometers, data-driven evidence on actual usage patterns is crucial for LCA analysis of SES. Second, country-specific resolved electricity carbon intensity data are rarely integrated into LCA of SES. This is a significant limitation, as the emissions associated with SES charging are highly related to the emission of electricity generation, which varies markedly across both countries and time. Failure to account for this heterogeneity can lead to misleading conclusions regarding LCA of SES. Third, the idle phase when e-scooters consume electricity without generating mobility benefits is frequently neglected in existing LCA. However, idle-phase electricity consumption, particularly in low-utilization fleets, may account for a considerable share of total electricity consumption. The magnitude of electricity wasted during idle periods, and its spatial variation across cities and countries, remains largely unquantified and considered in LCA.

In response to these gaps, this study adopts a comprehensive and data-driven approach. By leveraging multi-city operational data of SES, incorporating high-resolution electricity carbon intensity data at the country level, and explicitly modeling both in-use and idle phase emissions. This research aims to provide a more accurate, nuanced, and context-sensitive life cycle assessment of SES across Europe.

3. Method and data

3.1. Data

We employed a whole year of operational records from SES operated by two main operators (TIER and VOI) in 100 European cities (1 January–31 December 2022). The records fields contain detailed information of each trip of using SES in these cities including coordinates, time stamps, and battery State of Charge (SOC) at the starting and ending of a trip, retrieved via the official General Bikeshare Feed Specification API. Following the data-collection pipeline and quality-assurance procedures detailed in our previous work (Gao et al., 2024), we extracted trip-level information and partitioned the data into in-use and idle phases. Specifically, SOC during idle periods was logged at 5-min intervals, and for every detected trip the SOC change was captured by recording the last SOC value before the trip began and the SOC value at trip end. After filtering, the dataset contains $N = 47.3$ million valid trips with reliable SOC traces, forming the data basis for use-phase inventory modeling in Section 3.3.

3.2. Life cycle inventory

As depicted in Fig. 1, the LCA modeling follows the ISO 14040 standard (Huang et al., 2022), utilizing primary data from Ecoinvent (Hollingsworth et al., 2019) and empirical trip data. The adopted cradle-to-grave boundaries include four stages: primary material production, manufacturing, use phase, and EoL, tracking associated energy, materials, and emissions exchanges. All inventories are normalized to a functional unit per SES use, facilitating consistent comparisons across cities irrespective of differences in fleet utilization. The foreground system comprises the scooter (frame, battery, motor, electronics, tires, wiring), charger, and logistics necessary for SES operation. Background processes utilize Ecoinvent datasets, employing CML-2016 characterization factors. To reflect spatial variability, generic electricity grid assumptions are replaced with country-specific electricity mixes from 2022 as shown in Table 4.

Primary materials including virgin aluminum, steel, plastics, and NMC-111 lithium-ion cells dominate the SES mass balance, while recycled materials are credited according to supplier data. Material extraction, refining, fabrication energy, and direct process emissions are accounted for explicitly. Auxiliary materials such as lubricants and surface coatings are each individually below the ISO 14044 cut-off threshold of 1% of total mass or energy and are therefore excluded. During daily operation, the SES fleet incurs propulsion electricity consumption, idle-mode energy losses, and additional energy use (diesel or electricity) for nightly scooter collection, depot charging, and morning redeployment. Routine maintenance activities, mainly involving tire, brake, and electronics replacements, contribute approximately 1% to the total global warming potential (GWP). At retirement, SES are dismantled within the EU, where aluminum and steel recycling achieve recovery rates of 90% and 85%, respectively. Battery materials are recycled hydroelectrically in compliance with the 2023 EU Battery Regulation, achieving a 70% recovery rate. Secondary metal production offsets primary metal production, generating avoided-burden credits subtracted from the EoL inventory.

As shown in Fig. 1, The overall LCA framework transparently attributes GWP impacts across lifecycle stages, highlighting critical mitigation strategies including increased recycled material content, lightweighting, low-carbon energy sourcing for manufacturing, optimized charging logistics, and improved EoL material recovery. Material and energy usage data for SES production were collected

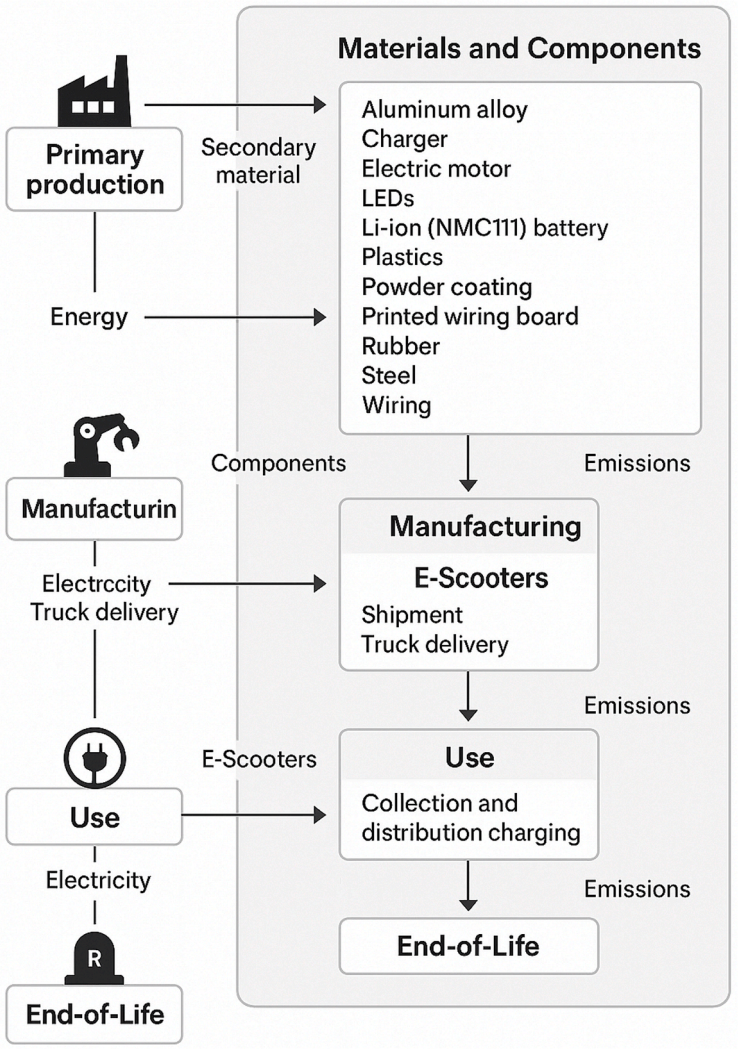

Fig. 1. Framework of life cycle assessment of SES.

from manufacturers, distributors, and existing literature. Each SES typically weighs approximately 13 kg, detailed further in Table 3. While auxiliary materials such as lubricants and paints are utilized during manufacturing, their overall quantities per scooter are minimal and therefore excluded based on the trade-off principle.

The overall LCI calculation is presented in Equation (1):

$$\mathrm{LCI} = \mathrm{LCI}_{\mathrm{production}} + \mathrm{LCI}_{\mathrm{shipping}} + \mathrm{LCI}_{\mathrm{use}} + \mathrm{LCI}_{\mathrm{EoL}} \tag{1}$$

where $\mathrm{LCI}_{\mathrm{production}}$ represents e-scooter manufacturing LCI including material extraction, components manufacturing, and final assembly of the scooter and corresponding battery inventory components, $\mathrm{LCI}_{\mathrm{shipping}}$ is associated with the transport of the e-scooter to the operation city, mainly includes the LCI of shipping and daily operation, $\mathrm{LCI}_{\mathrm{use}}$ associated with the electricity consumption, and $\mathrm{LCI}_{\mathrm{EoL}}$ stands for the disposal and end of life LCI regarding the lifelong emission.

According to the data-driven estimation of the use phase $\mathrm{LCI}_{\mathrm{use}}$, we further set $\mathrm{LCI}_{\mathrm{static}} = \mathrm{LCI}_{\mathrm{production}} + \mathrm{LCI}_{\mathrm{shipping}} + \mathrm{LCI}_{\mathrm{EoL}}$, thus the total LCI is represented by

$$\mathrm{LCI} = \mathrm{LCI}_{\mathrm{static}} + \mathrm{LCI}_{\mathrm{use}} \tag{2}$$

3.3. Use and idle phase inventory

We model the life cycle inventory for the use phase $\mathrm{LCI}_{\mathrm{use}}$, as the sum of distance-related and time-related contributions,

$$\mathrm{LCI}_{\mathrm{use}} = e^{\mathrm{ride}}\, d_{\mathrm{mileage}} + e^{\mathrm{idle}}\, t_{\mathrm{time}} \tag{3}$$

where

Table 3
Material components, percentage shares and material mass for e-scooter.

Material Components	Percentage Shares	Material Mass (kg)
Aluminium alloy	44.15%	5.73
Steel alloy	10.33%	1.33
Rubber	8.74%	1.13
Polycarbonate	2.0%	0.26
Lithium-ion battery pack	17.17%	2.23
Electric motor	8.75%	1.13
E-scooter charger	3.0%	0.39
Wiring steel	1.0%	0.13
Electronic components	3.73%	0.49
Tap water and additional plastic parts	1.46%	0.19
Total	100%	13

- d_{mileage} is the total distance travelled (km);
- t_{time} is the total operating time (h);
- e^{ride} is the use phase inventory intensity per unit distance (kg CO_2-eq km^{-1});
- e^{ride} is the idle phase inventory intensity per unit time (kg CO_2-eq h^{-1}).

To quantify uncertainty and variation in usage patterns, we derive empirical distributions for d_{mileage} and t_{time} from operational field data. We then apply Monte Carlo simulations to sample from these distributions. The reported LCI_{use} is the expected mean value derived from these simulations.

3.3.1. In-use electricity consumption estimation

We estimate electricity consumption during active use by identifying valid trips from sequential vehicle availability records. For each trip j, the associated SOC change (ΔSOC) is calculated as:

$$\Delta\text{SOC}_{\text{ride},\,j} = \text{SOC}_{\text{start},\,j} - \text{SOC}_{\text{end},\,j} \tag{4}$$

Invalid trips are excluded based on the following criteria:

- Trip distances shorter than 50 m or durations less than 60 s;
- Trips exhibiting SOC increases (negative ΔSOC);
- Trips with speeds exceeding 20 km/h or durations longer than 1 h.

For every valid trip an energy-per-kilometer term e_j^{ride} is computed,

$$e_j^{\text{ride}} = \frac{\Delta\text{SOC}_{\text{ride},j}\, C}{\eta\, d_j}, \tag{5}$$

with battery capacity $C = 0.5\,\text{kWh}$ and grid-to-wheel efficiency $\eta = 0.99$. We then aggregate these terms by vehicle v and day of data d , yielding the daily distance-weighted average in-use intensity as follows:

$$\bar{e}_{v,d}^{\text{ride}} = \frac{\sum_{j\in(v,d)} e_j^{\text{ride}}\, d_j}{\sum_{j\in(v,d)} d_j} \tag{6}$$

These daily averaged intensities $\bar{e}_{v,d}^{\text{ride}}$ form an empirical distribution for subsequent Monte Carlo simulations.

3.3.2. Idle energy loss estimation

Idle intervals are identified between consecutive trips for the same scooter, where spatial displacement is less than 50 m. For each idle interval k, the SOC reduction is computed as:

$$\Delta\text{SOC}_{\text{idle},k} = \text{SOC}_{\text{start},k} - \text{SOC}_{\text{end},k} \tag{7}$$

Idle intervals are excluded if:

- $\Delta\text{SOC}_{\text{idle},k} < 0$, indicating charging or battery swap events;
- $\Delta\text{SOC}_{\text{idle},k} > 20\%$, indicating measurement anomalies;
- Interval duration $t_k < 10\,\text{minutes}$.

For each valid idle interval, we compute hourly idle energy loss:

$$e_k^{\text{idle}} = \frac{\Delta\text{SOC}_{\text{idle},k}\, C}{\eta\, t_k} \tag{8}$$

Table 4
Electricity emission factors by country (g CO_2-eq/kWh).

Country	Emission	Country	Emission
Austria	85	Italy	225
Finland	40	Netherlands	263
France	50	Poland	614
Germany	329	Slovakia	84
Hungary	154	Sweden	8

We then calculate daily average idle intensities per scooter v as:

$$\bar{e}^{\text{idle}}_{v,d} = \frac{\sum_{k\in(v,d)} e^{\text{idle}}_k t_k}{\sum_{k\in(v,d)} t_k} \tag{9}$$

These daily averages $\bar{e}^{\text{idle}}_{v,d}$ constitute the empirical distribution of idle intensity per hour for Monte Carlo simulations.

3.3.3. Monte Carlo simulation

We conduct a Monte Carlo simulation to incorporate variability in unit intensities, daily mileage, idle durations, and service lifespan into the final LCI estimate. The simulation procedure involves the following detailed steps. For each Monte Carlo iteration i:

- Sample daily ride intensity $e^{(i)}_{\text{ride}}$ from empirical distribution $\{\bar{e}^{\text{ride}}_{v,d}\}$.
- Sample daily idle intensity $e^{(i)}_{\text{idle}}$ from empirical distribution $\{\bar{e}^{\text{idle}}_{v,d}\}$.
- Sample daily travel distance $M^{(i)}$ from empirical distribution of daily mileage.
- Sample daily idle duration $H^{(i)}$ from empirical distribution of daily idle hours.
- Compute annualized distance and idle time by scaling from the monitoring time window days T and estimated lifespan L (years):

$$d^{(i)}_{\text{annual}} = \frac{365}{T} M^{(i)}, \quad t^{(i)}_{\text{annual}} = \frac{365}{T} H^{(i)} \tag{10}$$

- Calculate total emissions for ride and idle phases over scooter lifetime as:

$$\text{LCI}^{(i)}_{\text{ride}} = e^{(i)}_{\text{ride}}\, d^{(i)}_{\text{annual}}, \quad \text{LCI}^{(i)}_{\text{idle}} = e^{(i)}_{\text{idle}}\, t^{(i)}_{\text{annual}} \tag{11}$$

Thus, total use-phase inventory for iteration i is:

$$\text{LCI}^{(i)}_{\text{use}} = \text{LCI}^{(i)}_{\text{ride}} + \text{LCI}^{(i)}_{\text{idle}} \tag{12}$$

We repeat the simulation $N = 10,000$ times to establish a robust statistical characterization of LCI_{use}. From the resulting distribution, we report the expected mean value alongside its 5–95 % confidence interval and standard deviation. :

$$\mathbb{E}[\text{LCI}_{\text{use}}] = \frac{1}{N}\sum_{i=1}^{N} \text{LCI}^{(i)}_{\text{use}} \tag{13}$$

3.3.4. LCA emission factor

Furthermore, Table 4 summarizes country-specific electricity emission facotrs by CO_2-eq. By combining this to Eqs. (3)–(13) and sampling the empirical distributions, we obtain a robust and data-driven estimation of the use phase LCI_{use}. This approach ensures that real-world variability in operational characteristics is comprehensively reflected in the final life cycle inventory assessment. The LCA emission factor (EF) is derived as:

$$\text{EF} = \frac{\text{LCI}_{\text{static}} + \text{LCI}_{\text{use}}}{L \times \bar{M} \times \bar{N}} \tag{14}$$

where L is the estimated lifespan (3 years), and $\bar{M}, \bar{N}$ is the mean trip distance and frequency.

4. Result

This section presents the results of our analysis of SES electricity consumption, starting from introducing the SES usage frequency intensity and trip distance distribution. Moreover, we focus on both in-use and idle phases, followed by a comparative assessment at the city level. We then incorporate country-specific electricity mix intensities to conduct a detailed LCA of SES operations, distinguishing among different constant carbon intensity factors. Finally, a sensitivity analysis is performed to evaluate the influence of key parameters derived from real-world trip data, with the aim of identifying effective strategies for reducing GHG emissions.

Table 5
List of cities analyzed.

City	Country	City	Country	City	Country
Aachen	Germany	Meerbusch	Germany	Bordeaux	France
Augsburg		Mönchen-gladbach		Bourgoin-Jallieu	
Berlin		Münster		Grenoble	
Bielefeld		Oldenburg		Lyon	
Bochum		Osnabrück		Marseille	
Bonn		Paderborn		Roubaix	
Bremen		Potsdam		Saint-Quentin-en-Yvelines	
Chemnitz		Recklinghausen		Budapest	Hungary
Cologne		Reutlingen		Eindhoven	Netherlands
Darmstadt		Rostock		Utrecht	
Dortmund		Saarbrucken		Gdańsk	Poland
Düsseldorf		Solingen		Gorzów Wielkopolski	
Erlangen		Stuttgart		Kołobrzeg	
Essen		Wolfsburg		Kraków	
Flensburg		Zwickau		Słupsk	
Frankfurt		Odense	Denmark	Szczecin	
Fürth		Borås		Warsaw	
Gelsenkirchen		Eskilstuna		Helsinki	Finland
Halle-Saale		Gothenburg		Lahti	
Hamburg		Halmstad		Tampere	
Hannover		Helsingborg		Turku	
Heilbronn		Jönköping		Innsbruck	Austria
Herford		Karlstad		Klagenfurt	
Hildesheim		Linköping	Sweden	Linz	
Ingolstadt		Lund		Málaga	Spain
Kaiserslautern		Malmö		Sevilla	
Karlsruhe		Norrköping		Milan	Italy
Kassel		Örebro		Modena	
Kiel		Stockholm		Monza	
Leipzig		Uppsala		Palermo	
Lübeck		Västerås		Reggio Emilia	
Wiesbaden		Bratislava	Slovakia	Turin	
Mainz		Brussels	Belgium		
Mannheim-Ludwigshafen		Namur			

4.1. SES usage pattern indicators

Based on the trip-level data extracted from the GBFS feeds of SES, we analyzed detailed usage patterns across 100 cities (shown in Table 5) by reconstructing individual trips from the start and end status of each vehicle. Figs. 2 and 3 illustrate the distribution and country-level variation in two key usage indicators: the daily utilization frequency and the average trip distance.

It is important to note that the spatial coverage of our dataset is uneven, with a greater number of cities represented in Germany, Sweden, and France. As a result, these countries exhibit smoother and more statistically stable distributions in both utilization frequency and trip distance. In contrast, countries such as Austria and the Netherlands are represented by a smaller portion of cities, which is caused by regulation limitations. It leads to distinctive, and sometimes multimodal, distribution shapes that reflect localized operational heterogeneity.

As shown in Fig. 2, daily utilization frequency varies considerably across countries, ranging from just 1.66 trips per vehicle in Slovakia to a peak of 4.06 in the Netherlands, representing a 2.4 fold difference. This wide variability suggests that the intensity of SES usage is highly context-dependent and may be influenced by factors such as urban density, SES operational service, policy support, or modal integration. These differences notably affect usage patterns and, by extension, contribute to variability in LCA outcomes. Furthermore, several countries display clearly skewed or bimodal frequency distributions, potentially indicating the presence of heterogeneous operational clusters or variations in service models within the same national context. In contrast, Fig. 3 reveals that average trip distance exhibits a much narrower range of variation, from 1,235 meters in the Netherlands to 1,904 meters in Spain. This suggests that while the number of trips per day is highly elastic across contexts, the physical length of each trip remains more stable, possibly constrained by consistent user travel behavior, urban infrastructure limitations, or pricing structures.

These findings indicate that differences in SES usage intensity across Europe are driven more by frequency of trips than by trip distance. From an SES operational and LCA perspective, this distinction is critical, as it implies that emissions and system efficiency are more sensitive to how frequently a vehicle is used rather than how far it travels per trip.

4.2. In-use and idle phase comparison

Apart from the trip usage indicators, the electricity consumption of SES is also estimated as battery SOC changes by estimating each trip based on the start and end status. Employing the assumption and method mentioned in Section 3.3 we calculated the

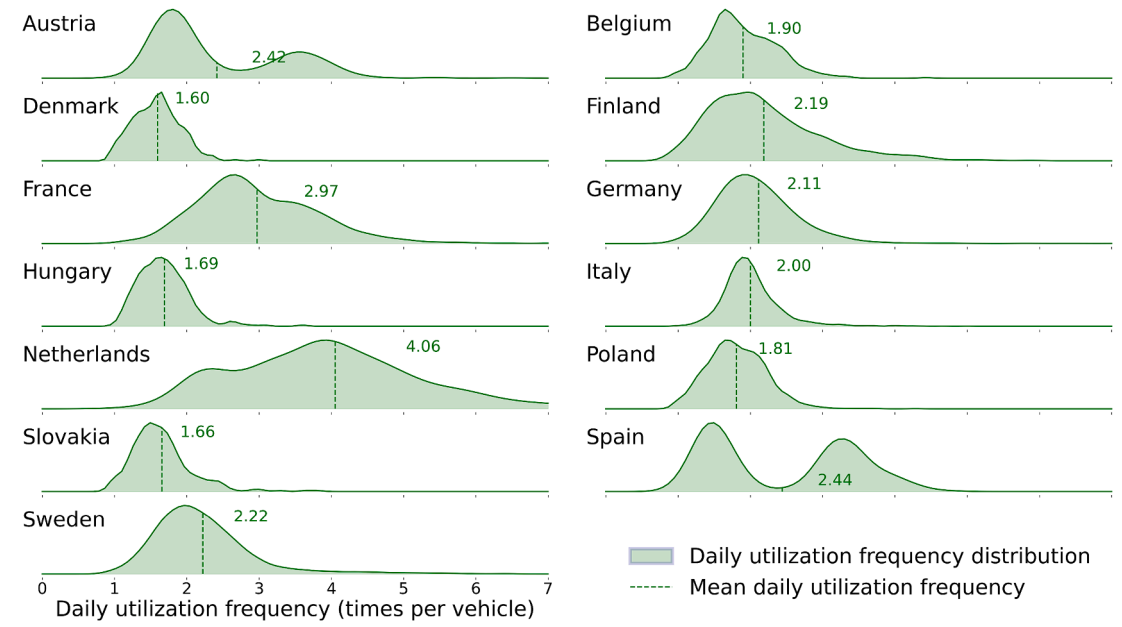

Fig. 2. Distribution and mean daily utilization frequency in country level comparison.

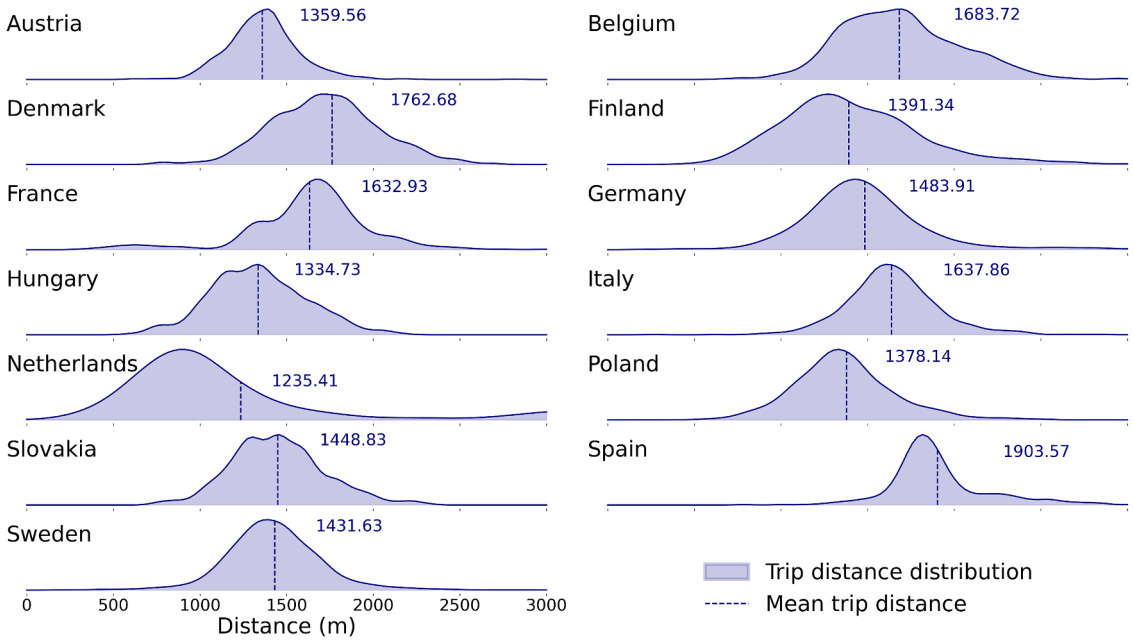

Fig. 3. Distribution and mean trip distance in country level comparison.

electricity consumption of in-use and idle phase as summarized in Fig. 4. In-use consumption is unimodal yet distinctly right-skewed as shown in Fig. 4(a), roughly 60 % of the study cities cluster between 12 and 16 Wh km^{-1}, the sample mean equals 15.94 Wh km^{-1}, and the 90 % interval stretches from about 11.5 to 22.5 Wh km^{-1}. Consequently, the most energy-intensive fleets require nearly twice the propulsion energy per kilometer of the most efficient ones, and a disparity attributable to differences in vehicle generation, driving-cycle aggressiveness, terrain and battery state-of-health. For a representative 0.5 kWh battery this translates to a depletion of 3.5 % SOC per km in the best-performing settings versus almost 7 % SOC per km in the worst.

Regarding the idle phase electricity consumption, it exhibits a much tighter spread as shown in Fig. 4(b). The mean electricity consumption is 1.49 Wh h^{-1}, and 90 % of cities fall within 1.1 to 2.1 Wh h^{-1}, suggesting broadly similar electronic hardware and heartbeat frequencies. Although such absolute differences are subtle, the accumulated electricity consumption over long parking periods might be significant. For example, at the average utilization of 2-3 trips per day, implying around 22 hour idle phase daily,

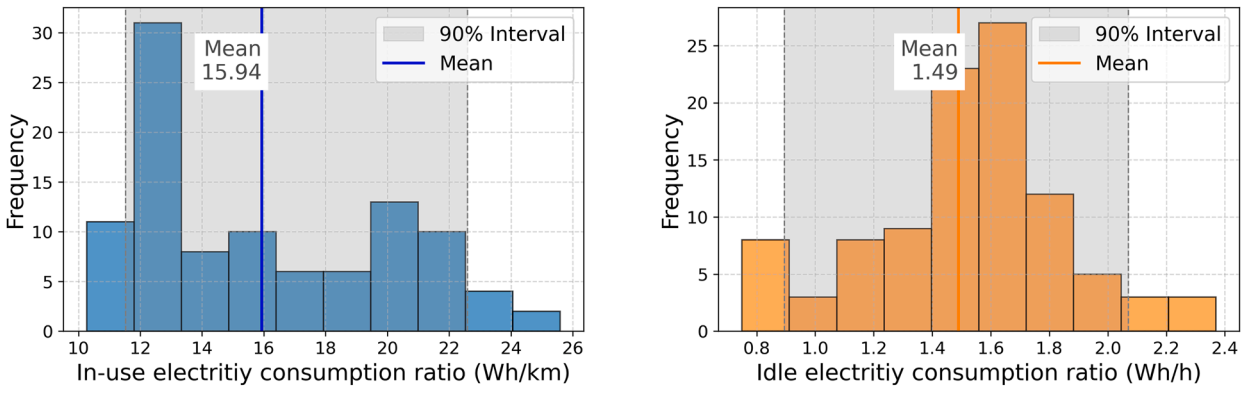

(a) In-use phase (b) Idle phase

Fig. 4. Distribution of electricity consumption among different cities.

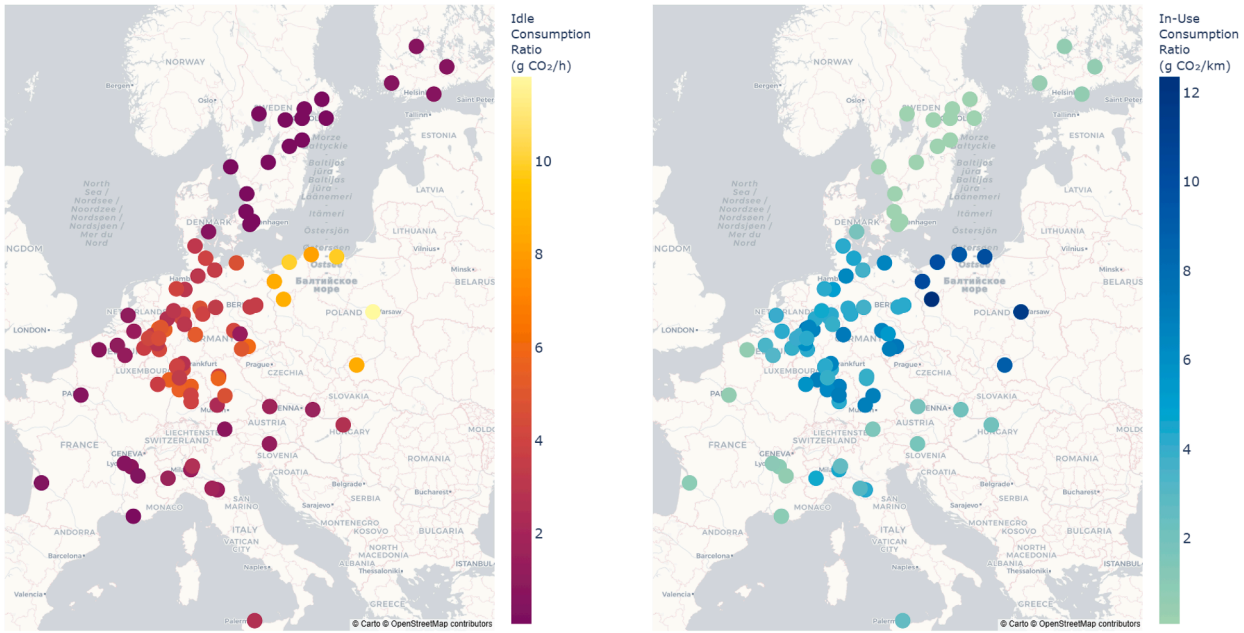

(a) Idle phase (g CO_2-eq/hour) (b) In-use phase (g CO_2-eq km^{-1})

Fig. 5. SES electricity consumption in Idle and In-use step among cities in Europe.

raises roughly 11.4 kWh of annual electricity consumption per scooter, an amount equivalent to the energy needed to ride roughly 715 kilometers at the mean in-use efficiency. In some cities with low-utilization contexts, where scooters may sit idle for most of the day, idle losses can therefore rival or even exceed in-use energy. Policies that raise trip frequency, thereby shortening idle durations, or that further reduce electronics power budgets, can deliver meaningful life cycle GHG savings, especially in regions where the electricity mix is already largely decarbonized.

By applying the electricity LCA emission factors for each city, we have then quantified and compared spatial variations in environmental impact across Europe. As shown in Fig. 5, overall, Northern and Southern European regions exhibit relatively low emission factors, reflecting their reliance on cleaner electricity mixes. In contrast, Central European cities display substantially higher factors, with Eastern Europe following a similar pattern. This disparity is driven primarily by higher grid-carbon intensity, which amplifies both idle and in-use emissions beyond expectations.

For instance, as shown in Fig. 5(a), the idle phase emission in Warsaw reaches approximately 12.13 g CO_2-eq h^{-1} two to three orders of magnitude greater than in Malmö (0.053 g CO_2-eq h^{-1}) or Stockholm (0.034 g CO_2-eq h^{-1}). A comparable pattern occurs during the in-use phase as shown in Fig. 5(b), Szczecin records 11.17 g CO_2-eq km^{-1} and Gelsenkirchen 7.84 g CO_2-eq km^{-1}, whereas cities such as Västerås (0.092 g CO_2-eq km^{-1}) and Roubaix (0.63 g CO_2-eq km^{-1}) remain two to three orders of magnitude lower.

These results underscore the critical influence of electricity-sector de-carbonization on both standby and operational emissions of SES.

Apart from the city level comparison, silimiarity can be found in the same country. We further compare these country-level distingished result as shown in Fig. 6(a), Fig. 6(b) and Table 6. Significant variation is observed among countries in both battery consumption and associated GHG during in-use and idle phases. Slovakia (5.12 SOC km^{-1}), Belgium (4.49 SOC km^{-1}) and Austria (4.05 SOC km^{-1}) exhibit the highest in-use battery depletion rates, whereas Sweden (2.66 SOC km^{-1}) and Finland (2.80 SOC km^{-1}) record the lowest values. These disparities likely reflect differences in vehicle efficiency, weather conditions and driving speed profiles across regions, besides, Central European road networks, characterized by more complex terrain and higher average velocities, tend to incur greater energy losses per kilometer, while the predominance of advanced electric vehicle models and milder driving environments in the Nordic countries contributes to reduced battery usage.

With respect to in-use carbon intensity Poland (10.36 g CO_2–eq km^{-1}) far exceeds all other nations, followed by Germany (5.30 g CO_2–eq km^{-1}) and the Netherlands (4.18 g CO_2–eq km^{-1}). In contrast, Sweden (0.11 g CO_2–eq km^{-1}) and Finland (0.56 g CO_2–eq km^{-1}) demonstrate markedly lower footprints. This pattern is principally attributable to variations in national electricity-generation portfolios, reliance on coal and natural gas in Poland and Germany yields higher marginal emission factors, whereas the heavy deployment of hydroelectric and nuclear power in Sweden and Finland effectively minimizes CO_2 emissions during vehicle operation.

During idle periods, both energy draw and emissions decline substantially relative to active driving, yet the relative national rankings remain consistent. Finland (0.39 SOC/h) and Hungary (0.32 SOC/h) show the greatest standby battery consumption, while Denmark (0.17 SOC/h) and Sweden (0.28 SOC/h) lie at the lower end of the spectrum. Idle-phase emissions are highest in Poland (0.95 g CO_2–eq h^{-1}) and Germany (0.51 g CO_2–eq h^{-1}), whereas the Swedish near-zero value (0.01 g CO_2–eq h^{-1}) underscores the advantages of a low-carbon grid even when vehicles are not in motion.

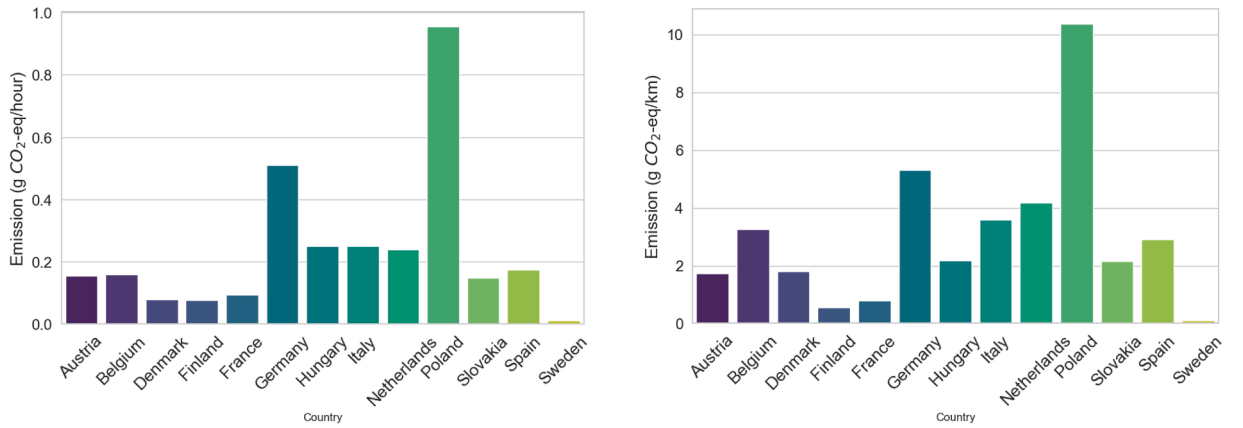

(a) Idle electricity consumption (g CO_2-eq/hour) (b) In-use electricity consumption (g CO_2-eq km^{-1})

Fig. 6. Country level SES emission factor comparison (g CO_2-eq km^{-1}).

Table 6
Battery Use and Power Consumption in In-use and Idle Phases for Different Countries.

Country	In-Use Phase Battery Use (SOC km^{-1})	Idle Phase Battery Use (SOC/h)	In-Use Phase Consumption (g CO_2-eq km^{-1})	Idle Phase Consumption (g CO_2-eq h^{-1})
Austria	4.05	0.36	1.72	0.15
Belgium	4.49	0.22	3.25	0.16
Denmark	3.81	0.17	1.79	0.08
Finland	2.80	0.39	0.56	0.08
France	3.14	0.38	0.78	0.10
Germany	3.22	0.31	5.30	0.51
Hungary	2.82	0.32	2.17	0.25
Italy	3.18	0.22	3.58	0.25
Netherlands	3.18	0.18	4.18	0.24
Poland	3.38	0.31	10.36	0.95
Slovakia	5.12	0.35	2.15	0.15
Spain	3.68	0.22	2.91	0.17
Sweden	2.66	0.28	0.11	0.01

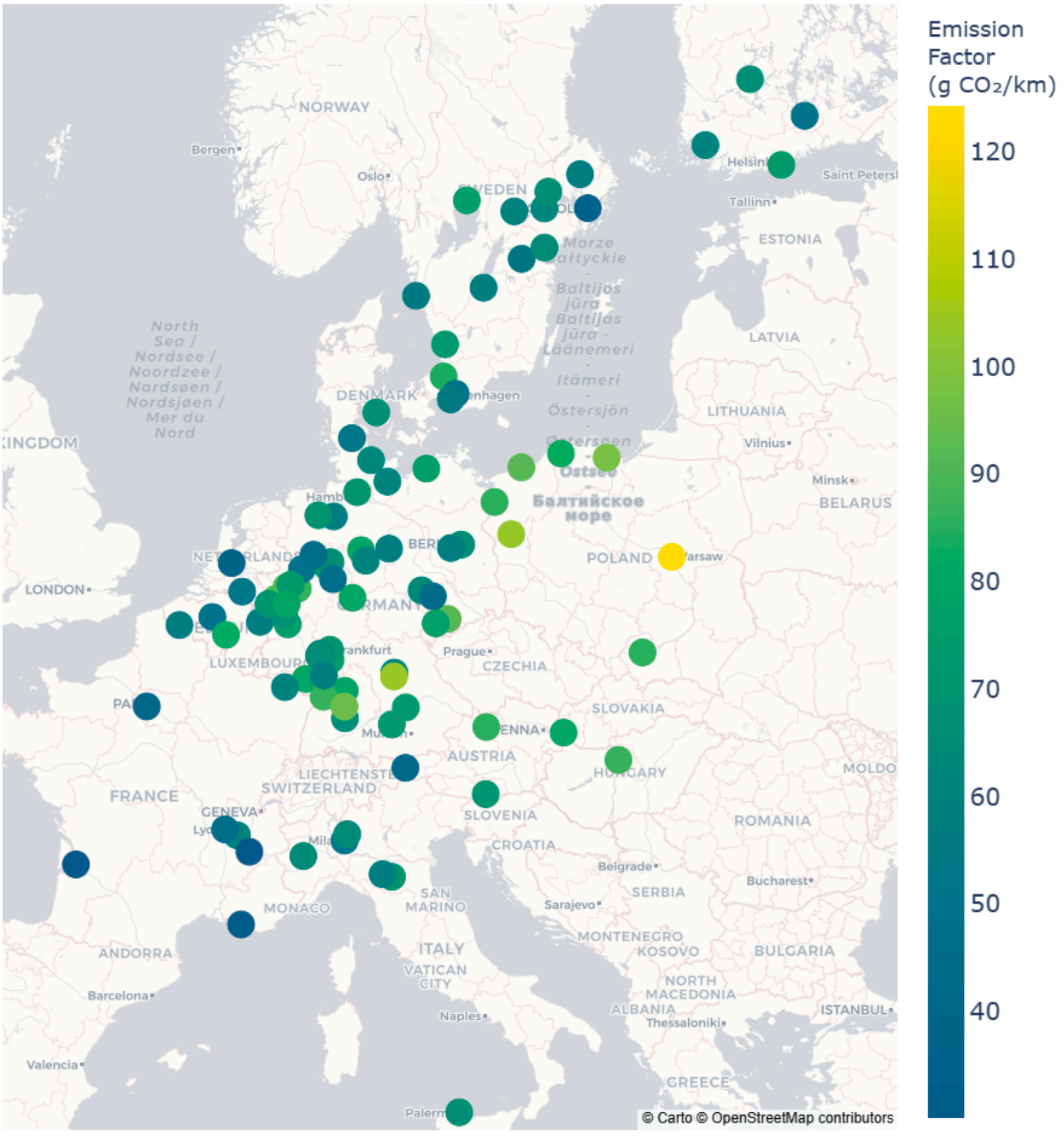

Fig. 7. Average SES emission factor among cities in Europe (g CO_2-eq km^{-1}).

4.3. LCA result

As defined in Section 3.3, sourced from Hollingsworth et al. (2019) and using the LCA method Ecoinvent - CML v4.8 2016, the GWP of SES in production, shipping and end of life is supposed to be the same, which is calculated as follow

$$LCI_{static} = LCI_{production} + LCI_{shipping} + LCI_{EoL} = 115.644 \text{ kg } CO_2\text{-eq} \quad (15)$$

By aggregating the overall life cycle emission, the emission factor of European cities can be summarized as shown in Fig. 7, with darker blue tones indicating lower carbon intensities and yellow indicating higher values Table 7. A pronounced north–south/east–west gradient is evident. Specically, with detailed estimated emission factors shown in Table 8, Nordic cities such as Stockholm (35.14 g CO_2-eq km^{-1}), Helsinki (73.80), and Gothenburg (56.26) consistently exhibit lower emission factors, largely due

Table 7
Average emission factors by city (g CO_2-eq km^{-1}).

City	Emission Factor	City	Emission Factor	City	Emission Factor
Aachen	59.18	Meerbusch	89.85	Bordeaux	30.34
Augsburg	72.73	Mönchen-gladbach	70.50	Bourgoin-Jallieu	61.47
Berlin	65.84	Münster	50.80	Grenoble	30.08
Bielefeld	70.43	Oldenburg	69.76	Lyon	45.50
Bochum	119.66	Osnabrück	47.10	Marseille	30.86
Bonn	75.59	Paderborn	47.05	Roubaix	56.91
Bremen	58.34	Potsdam	57.75	Saint-Quentin-en-Yvelines	39.96
Chemnitz	91.41	Recklinghausen	74.30	Budapest	86.90
Cologne	68.10	Reutlingen	66.44	Eindhoven	51.51
Darmstadt	76.30	Rostock	75.88	Utrecht	37.13
Dortmund	85.92	Saarbrucken	60.56	Gdańsk	97.37
Düsseldorf	50.85	Solingen	79.25	Gorzów Wielkopolski	103.63
Erlangen	62.16	Stuttgart	95.88	Kołobrzeg	91.51
Essen	104.71	Wolfsburg	58.48	Kraków	85.68
Flensburg	51.72	Zwickau	77.63	Słupsk	82.93
Frankfurt	71.45	Odense	68.27	Szczecin	85.32
Fürth	104.16	Borås	54.77	Warsaw	124.34
Gelsenkirchen	91.83	Eskilstuna	62.50	Helsinki	73.80
Halle-Saale	64.22	Gothenburg	56.26	Lahti	49.54
Hamburg	70.47	Halmstad	72.22	Tampere	68.53
Hannover	79.03	Helsingborg	83.87	Turku	62.43
Heilbronn	80.12	Jönköping	58.78	Innsbruck	40.08
Herford	66.17	Karlstad	75.45	Klagenfurt	71.55
Hildesheim	61.78	Linköping	53.78	Linz	85.52
Ingolstadt	72.00	Lund	49.97	Málaga	67.17
Kaiserslautern	80.88	Malmö	55.26	Sevilla	33.16
Karlsruhe	87.10	Norrköping	64.40	Milan	51.85
Kassel	81.28	Örebro	59.72	Modena	69.69
Kiel	63.75	Stockholm	35.14	Monza	64.25
Leipzig	43.22	Uppsala	58.63	Palermo	66.57
Lübeck	60.80	Västerås	67.62	Reggio Emilia	58.18
Wiesbaden	61.89	Bratislava	80.89	Turin	65.04
Mainz	65.60	Brussels	49.38		
Mannheim-Ludwigshafen	57.67	Namur	82.11		

Table 8
Average daily trips, mean distance per trip, and corresponding emission factors by country.

Country	Trips (per day)	Distance (m)	Emission Factor (g CO_2-eq km^{-1})
Austria	2.42	1359.56	65.72
Belgium	1.90	1683.72	65.74
Denmark	1.60	1762.68	68.27
Finland	2.19	1391.34	63.57
France	2.97	1632.93	42.16
Germany	2.11	1483.91	71.38
Hungary	1.69	1334.73	86.90
Italy	2.00	1637.86	62.60
Netherlands	4.06	1235.41	44.32
Poland	1.81	1378.14	95.83
Slovakia	1.66	1448.83	80.89
Spain	2.44	1903.57	50.17
Sweden	2.22	1431.63	60.56

to their decarbonized electricity grids, and high SES usage indicators. Similarly, several Western European cities, including Paris, Bordeaux, Amsterdam, and Lyon, fall within the low range of 30–60 g CO_2-eq km^{-1}, reflecting a relatively favorable combination of grid emissions intensity and operational efficiency.

In contrast, cities in Central Europe and the Benelux region tend to cluster in the mid-range (60–80 g CO_2-eq km^{-1}). For example, Cologne (68.10) and Darmstadt (76.30) represent cities where moderately carbon-intensive power supplies and logistic systems yield intermediate emission factors. These cities often benefit from relatively high vehicle usage indicators but may be constrained by grid mix or suboptimal fleet rebalancing practices.

At the high end of the spectrum, emission factors exceed 90 g CO_2-eq km^{-1} in several Eastern and Southern European cities. Notably, Warsaw stands out with the highest observed value of 124.34 g CO_2-eq km^{-1}, primarily due to the carbon-intensive nature of Poland's electricity generation and relatively low trip frequency. Other high-emission cities include Bochum (119.66 g CO_2-eq

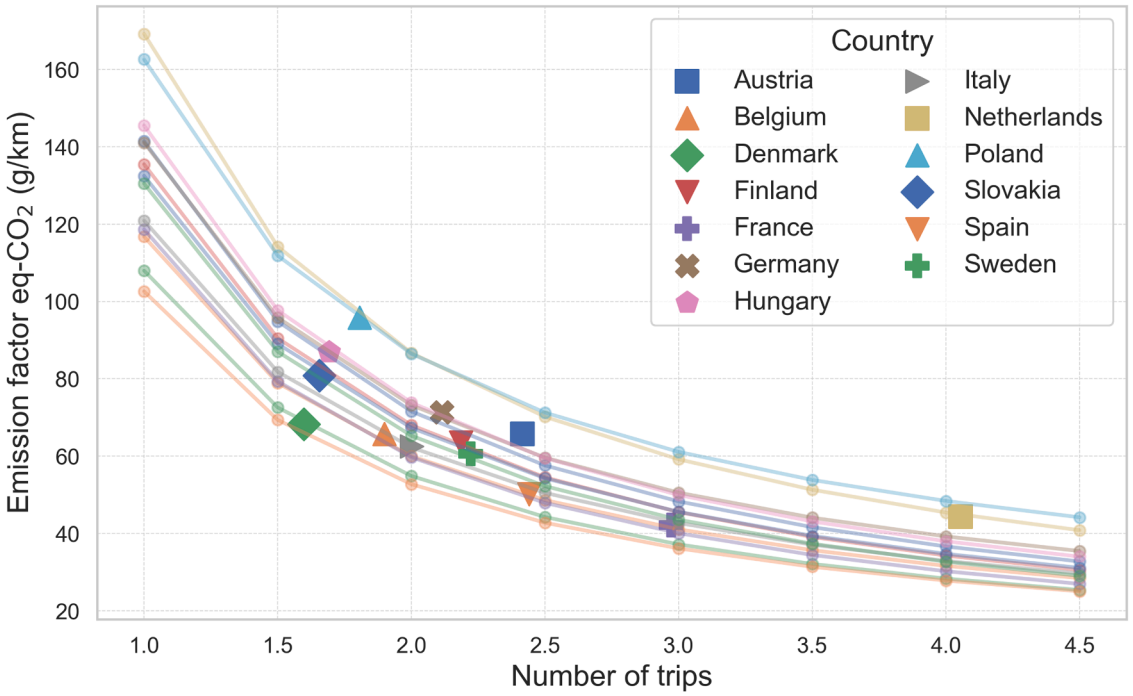

Fig. 8. Estimated emission factor by changing number of trips.

km^{-1}), Essen (104.71 g CO_2-eq km^{-1}), and Gorzów Wielkopolski (103.63 g CO_2-eq km^{-1}), reflecting both carbon-heavy energy supply and underutilized scooter fleets. In Southern Europe, cities like Milan (51.85 g CO_2-eq km^{-1}) and Palermo (66.57 g CO_2-eq km^{-1}) fall in the mid-to-high range, with slightly improved performance compared to their Eastern counterparts but still significantly above the Nordic average.

While aggregating the SES factors into country-levle, owing to theexceptionally high trip count, the Netherlands combines intensive fleet utilization with a comparatively low electricity-mix carbon intensity, thereby attaining the most favorable final emission factor (44.32 g CO_2-eq km^{-1}). A similar coupling of high utilization efficiency and low-carbon electricity is observed in France (42.16 g CO_2-eq km^{-1}), Spain (50.17 g CO_2-eq km^{-1}) and Sweden (60.56 g CO_2-eq km^{-1}), underscoring the importance of both operational intensity and grid de-carbonization in minimizing per-kilometer impacts.

The dispersion in emission factors is nevertheless substantial, with coal-reliant Poland recording 95.83 g CO_2-eq km^{-1}, which is more than double the Dutch value, while Slovakia (80.89 g CO_2-eq km^{-1}) and Hungary (86.90 g CO_2-eq km^{-1}) exhibit relatively modest trip frequencies yet elevated electricity-related emissions. These results corroborate the decisive influence of electricity-mix carbon intensity on the operational footprint of electric micro-mobility, vehicles operated in grids dominated by fossil fuels incur far greater climate burdens per kilometer than identical vehicles powered by low-carbon sources. Consequently, without concurrent progress in grid de-carbonization, increased deployment of SES fleets in carbon-intensive regions may erode or even negate the life cycle benefits otherwise expected from electrified urban transport.

4.4. Sensitivity analysis

A sensitivity analysis was conducted to quantify how variations in key operational parameters propagate through the LCA of SES. For each parameter examined, its value was systematically varied while all other parameters were fixed at baseline conditions, hence the resulting emission factor isolates the marginal effect attributable solely to the parameter under scrutiny.

Fig. 8 illustrates the non-linear relationship between daily trip frequency and the life cycle emission factor. For the thirteen study countries, the response curve is sharply convex, increasing utilization from one to two trips per day lowers the median emission factor from roughly 96 to 58 g CO_2-eq km^{-1}, a 40% decline, whereas a comparable increment from four to five trips yields a marginal improvement of around 5 g CO_2-eq km^{-1}. The largest absolute gain occurs in Poland, where a coal-dominated electricity mix produces an initial factor of 95.8 g CO_2-eq km^{-1}, while raising utilization from 1.8 to 2.8 trips trims the factor to about 72 g CO_2-eq km^{-1}, underscoring how even modest operational improvements can offset a sizable share of overall emissions. The Netherlands exemplifies the converse mechanism, while its outstanding performance 44.3 g CO_2-eq km^{-1} is achieved almost entirely through an exceptionally high trip rate 4.06 per day, despite an electricity mix that is far from carbon-neutral and the shortest mean trip distance in the sample. Were its utilization to fall to the Polish level, the emission factor in Netherlands would approach 95 g CO_2-eq km^{-1}. France provides the benchmark case in which a low-carbon grid is coupled with above-average utilization, further increases in trip frequency yield only minor absolute gains, reflecting an already optimized configuration.

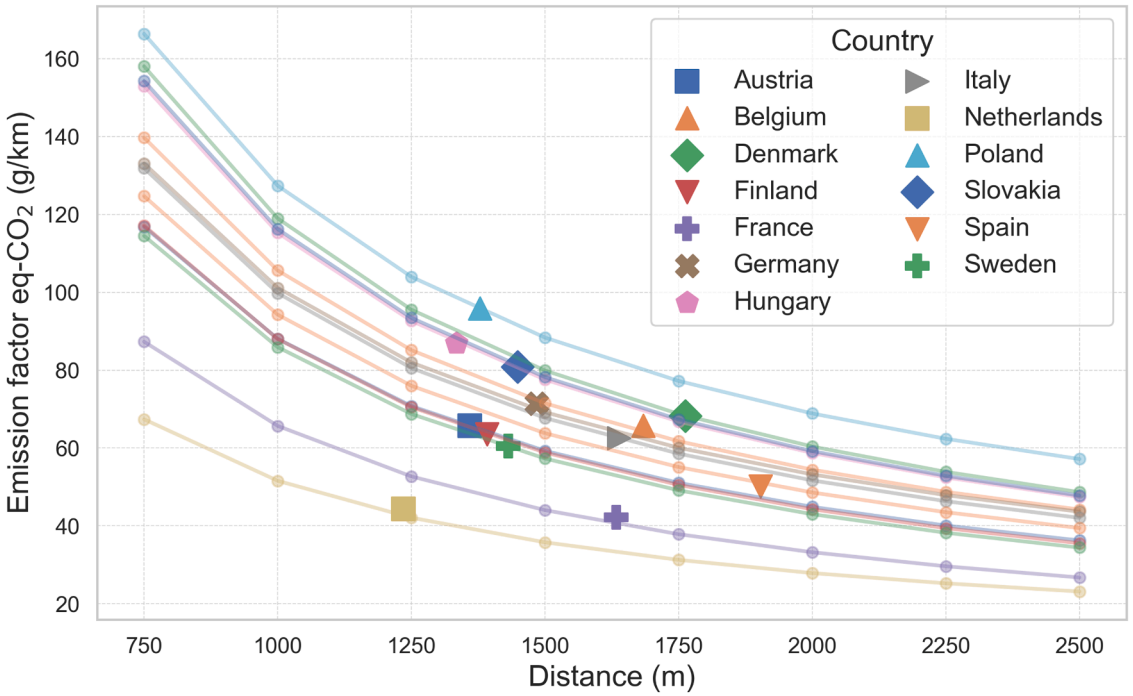

Fig. 9. Estimated emission factor by changing trip distance.

Fig. 9 depicts the sensitivity of the emission factor to mean trip distance. Extending the average trip distance from 0.75 to 1.50 g CO_2-eq km^{-1} nearly halves the median footprint. Countries with carbon-intensive grids such as Poland, Slovakia, and Hungary retain the highest factors across the full distance range, yet their curves remain steep, indicating substantial potential for mitigation via even moderate distance expansion. Practical instruments such as distance-based price discounts or zone re-design could therefore encourage longer, purpose-oriented rides, simultaneously increasing utilization and enhancing consumption impacts.

5. Discussion and conclusion

This paper has quantified the climate footprint of SES services in 100 European cities by means of a full life cycle assessment based on the Ecoinvent–CML v4.8 2016 inventory and GBFS trip data. Manufacturing, shipping and end-of-life treatment jointly impose an invariant burden of 115.6 kg CO_2-eq per vehicle. Whether this upfront load dominates total impacts depends almost entirely on how intensively the fleet is used and on the carbon content of the local electricity mix. The main insights are summarized some key points as follows:

1. For very low-carbon grids such as cities in Sweden and France, the average in-use and idle electricity translate into only around 0.09 g CO_2-eq km^{-1} and about 0.10 g CO_2-eq h^{-1}, respectively. In Warsaw, by contrast, the same scooter requires 15.94 Wh km^{-1} while moving and 1.49 W while idle, which under Poland's coal-intensive mix corresponds to 11.50 g CO_2-eq km^{-1} and 11.83 g CO_2-eq h^{-1}. The almost magnitude gap underscores that even in future decarbonized scenarios, non-trivial in-use and idle electricity demand must still be accounted for.
2. Cross-country usage patterns strongly condition life cycle results. Average daily utilization frequency ranges from 1.66 rides in Slovakia to 4.06 rides in the Netherlands, whereas mean trip distance varies only from 1 235 m (Netherlands) to 1 904 m (Spain). Because lifetime service distance scales directly with ride frequency, Poland, Hungary and Slovakia, each combining low utilization with carbon-intensive electricity, exhibit the highest life cycle GWPs, almost twice those of the Netherlands or France. These contrasts confirm that operational intensity and grid de-carbonization must advance together to minimize SES climate impacts.
3. Our sensitivity analysis indicates that trip frequency and average trip distance substantially influence per-kilometer emissions, with potential ±30% variation under realistic parameter ranges. The result shows that raising utilization from one to two rides per day cuts the median emission factor by about 40 %, whereas adding a fifth ride after the fourth lowers it by less than 5 g km^{-1}. Trip distance extensions still yield notable savings for well-performing countries, but for Poland, Hungary and Slovakia the most immediate and impactful lever is to boost ride frequency through dynamic rebalancing, pricing incentives or service-area redesign, thereby diluting the fixed production burden over a larger vehicle-kilometer base.

The following limitations should be acknowledged when interpreting our results and should guide future research. First, the life cycle inventory relies on Ecoinvent background data and assumes a uniform three-year service life; any divergence in component

sourcing, refurbishment schedules or premature fleet attrition could appreciably shift the embedded production burden, and collecting operator-specific primary data would improve estimates of material flows and failure rates. Second, national electricity-mix intensities were fixed at 2023 annual averages, thereby overlooking hourly and seasonal variability as well as prospective grid de-carbonization; integrating time-resolved or marginal-emission factors could provide a more realistic picture of operational impacts. Third, trip statistics are drawn from a single year of GBFS data and may not capture atypical weather, pandemic disruptions or long-term behavioral shifts, so multi-year panel datasets and extreme-event scenario tests should be pursued to strengthen robustness. Finally, the analysis addresses only greenhouse-gas emissions, leaving out other environmental and social externalities such as particulate matter, mineral depletion, noise and safety; adopting a multi-impact life cycle framework with both midpoint and endpoint indicators would broaden the sustainability appraisal. Addressing these gaps through richer data, dynamic modeling and a wider set of impact categories will yield a firmer evidence base for low-carbon micro-mobility policy.

CRediT authorship contribution statement

Ruo Jia: Writing – review & editing, Writing – original draft, Visualization, Validation, Methodology, Formal analysis, Data curation, Conceptualization; **Kun Gao:** Writing – review & editing, Supervision, Resources, Project administration, Investigation, Funding acquisition, Data curation.

Data availability

The authors do not have permission to share data.

References

Baumgartner, C., Helmers, E., 2024. Life cycle assessment of electric kick scooters: consolidating environmental impact quantification and concluding climate-friendly use options. Environ Sci Europe 36 (1), 96.

Brandt, J., Iversen, T., Eckert, C., Peterssen, F., Bensmann, B., Bensmann, A., Beer, M., Weyer, H., Hanke-Rauschenbach, R., 2024. Cost and competitiveness of green hydrogen and the effects of the european union regulatory framework. Nat Energy 9 (6), 703–713.

Calan, C., Sobrino, N., Vassallo, J.M., 2024. Understanding life-cycle greenhouse-gas emissions of shared electric micro-mobility: A systematic review. Sustainability 16 (13), 5277.

Dott, 2024. Dott 2023 sustainability report. Accessed: 2024-07-XX. https://ridedott.com/wp-content/uploads/2024/07/dott-2023-sustainability-report.pdf.

European Environment Agency, 2024. Greenhouse gas emission intensity of electricity generation in europe. https://www.eea.europa.eu/en/analysis/indicators/greenhouse-gas-emission-intensity-of-1. Accessed: 16 May 2025.

Gao, K., Jia, R., Liao, Y., Liu, Y., Najafi, A., Attard, M., 2024. Big-data-driven approach and scalable analysis on environmental sustainability of shared micromobility from trip to city level analysis. Sustain Cities Soc 115, 105803.

Gao, K., Yang, Y., Li, A., Li, J., Yu, B., 2021a. Quantifying economic benefits from free-floating bike-sharing systems: a trip-level inference approach and city-scale analysis. Transp Res part A Policy Pract 144, 89–103.

Gao, K., Yang, Y., Li, A., Qu, X., 2021b. Spatial heterogeneity in distance decay of using bike sharing: An empirical large-scale analysis in shanghai. Transp Res Part D Transp. Environ 94, 102814.

Gebhardt, L., Ehrenberger, S., Wolf, C., Cyganski, R., 2022. Can shared e-scooters reduce CO2 emissions by substituting car trips in germany? Transp Res Part D Transp Environ 109, 103328.

Hollingsworth, J., Copeland, B., Johnson, J.X., 2019. Are e-scooters polluters? the environmental impacts of shared dockless electric scooters. Environ Res Lett 14 (8), 084031.

Holmgren, K., Einarson Lindvall, E., Rosell, J., 2024. Life cycle assessment of shared dockless stand-up e-scooters in sweden. J Sustain Development Energy Water Environ Syst 12 (2), 1–18.

Hu, L., Liao, Y., Gao, K., Jin, S., Precup, R.-E., 2025. Integration of e-scooter sharing with public transit on employment accessibility and equity. Transportation Research Part D: Transport and Environment 140, 104604.

Huang, Y., Jiang, L., Chen, H., Dave, K., Parry, T., 2022. Comparative life cycle assessment of electric bikes for commuting in the UK. Transp Res Part D Transp Environ. 105, 103213.

Jia, R., Chamoun, R., Wallenbring, A., Advand, M., Yu, S., Liu, Y., Gao, K., 2023. A spatio-temporal deep learning model for short-term bike-sharing demand prediction. Electron. Res. Archive 31 (2), 1031–1047.

Kazmaier, M., Taefi, T.T., Hettesheimer, T., 2020. Techno-economical and ecological potential of electric scooters: a life cycle analysis. Eur J Transp Infrast Res 20 (4), 233–251.

Kolat, M., Tettamanti, T., Bécsi, T., Esztergár-Kiss, D., 2023. On the relationship between the activity at point of interests and road traffic. Commun Transp Res 3, 100102.

Kuang, S., Liu, Y., Wang, X., Wu, X., Wei, Y., 2024. Harnessing multimodal large language models for traffic knowledge graph generation and decision-making. Commun Transp Res 4, 100146.

Li, A., Zhao, P., Liu, X., Mansourian, A., Axhausen, K.W., Qu, X., 2022. Comprehensive comparison of e-scooter sharing mobility: Evidence from 30 european cities. Transp Res Part D Transp Environ 105, 103229.

Li, Y., Yang, X., Du, E., Liu, Y., Zhang, S., Yang, C., Zhang, N., Liu, C., 2024. A review on carbon emission accounting approaches for the electricity power industry. Appl Energy 359, 122681.

Liu, B., Liu, X., Yang, Y., Chen, X., Ma, X., 2023. Resilience assessment framework toward interdependent bus–rail transit network: Structure, critical components, and coupling mechanism. Commun Transp Res 3, 100098.

Moreau, H., de Jamblinne de Meux, L., Zeller, V., D'Ans, P., Ruwet, C., Achten, W. M.J., 2020. Dockless e-scooter: A green solution for mobility? comparative case study between dockless e-scooters, displaced transport, and personal e-scooters. Sustainability 12 (5), 1803.

Reis, A.F., Baptista, P., Moura, F., 2023. How to promote the environmental sustainability of shared e-scooters: A life-cycle analysis based on a case study from lisbon, portugal. J Urban Mobil 3, 100044.

Scarlat, N., Prussi, M., Padella, M., 2022. Quantification of the carbon intensity of electricity produced and used in europe. Appl Energy 305, 117901.

Schelte, N., Severengiz, S., Schünemann, J., Finke, S., Bauer, O., Metzen, M., 2021. Life cycle assessment on electric moped scooter sharing. Sustainability 13 (15), 8297.

Su, L., Yan, X., Zhao, X., 2024. Spatial equity of micromobility systems: A comparison of shared e-scooters and docked bikeshare in washington DC. Transp policy 145, 25–36.

Tranberg, B., Corradi, O., Lajoie, B., Gibon, T., Staffell, I., Andresen, G.B., 2019. Real-time carbon accounting method for the european electricity markets. Energy Strat Rev 26, 100367.

Voi, 2025. Publications. https://www.voi.com/publications. Accessed: 2025-05-19.
Weschke, J., Oostendorp, R., Hardinghaus, M., 2022. Mode shift, motivational reasons, and impact on emissions of shared e-scooter usage. Transportation Research Part D: Transport and Environment 112, 103468.
Zhu, Z., Lu, C., 2023. Life cycle assessment of shared electric bicycle on greenhouse gas emissions in china. Sci Total Environ 860, 160546.